Hindawi Publishing Corporation
International Journal of Photoenergy
Volume 2016, Article ID 4651654, 8 pages
http://dx.doi.org/10.1155/2016/4651654

Research Article

Influence of Anodization Time on Photovoltaic Performance of DSSCs Based on TiO_2 Nanotube Array

Jinghua Hu,[1,2] Shiwu Hu,[1] Yingping Yang,[1] Shengqiang Tong,[1] Jiejie Cheng,[1] Mengwei Chen,[1] Li Zhao,[2,3] and Jinxia Duan[3]

[1]*School of Science, Wuhan University of Technology, Wuhan 430070, China*
[2]*Department of Chemical and Petroleum Engineering, The University of Pittsburgh, Pittsburgh, PA 15261, USA*
[3]*Hubei Collaborative Innovation Center for Advanced Organic Chemical Materials, Faculty of Materials Science and Engineering, Hubei University, Wuhan 430062, China*

Correspondence should be addressed to Yingping Yang; ypyang@whut.edu.cn

Received 31 August 2016; Accepted 31 October 2016

Academic Editor: P. Davide Cozzoli

Highly ordered TiO_2 nanotube arrays (TNT arrays) were fabricated by two-step anodization process. In order to further improve the performance of DSSCs, TNT arrays were optimized by changing the anodization conditions to meet the requirements of high-performance photoanode. The photoelectric conversion properties of DSSCs based on P25/TNT arrays double-layer film with different anodization time were investigated and compared. The results show that the conversion efficiency of 4.20% was achieved in double-layer photoanode at 18 h, with an open-circuit voltage (V_{oc}) of 0.65 V and short-circuit current density (J_{sc}) of 9.98 mA cm^{-2}.

1. Introduction

At present, energy problem becomes one of the major problems that human being must confront. Solar energy is abundant and pollution-free and is not limited by the geographical environment and gradually becomes the main research object to solve the energy problem. In all solar cells, dye-sensitized solar cells (DSSCs) have attracted extensive attentions from the researchers all over the world due to their low production cost, simple preparation process, high conversion efficiency, and environment friendly properties [1–3].

Different from the traditional semiconductor solar cell, DSSCs are a new type of special structure, which consist of dye-sensitized nanocrystalline TiO_2 photoanode, redox electrolyte, and counter electrode [4–7]. TiO_2 photoanode is an important part of DSSCs and is closely related to light harvesting and electron injection and collection [8]. The dye molecules were adsorbed on the surface of nanocrystalline TiO_2, and the energy band structure of nanocrystalline TiO_2 is matched with dye molecule, so the electrons can be injected into the TiO_2 conduction band quickly and efficiently [9–12]. In order to obtain high efficiency DSSCs, the preparation of TiO_2 photoanode with excellent performance is essential.

So far, the research of nanocrystalline TiO_2 photoanode is mainly focused on the design of the morphology of TiO_2 [13–16]. A variety of one-dimensional (1D) TiO_2 structures with different micromorphology were prepared and applied to DSSCs, such as TiO_2 nanorods [17], TiO_2 nanowires [18], and TiO_2 nanotubes [19]. Compared with other TiO_2 structures, TiO_2 nanotube arrays (TNT arrays) have the characteristics of the vertical hollow structure, which greatly promote the electronic transmission in photoanode [20, 21]. In 2001, Gong et al. first synthesized TNT arrays by anodic oxidation reactions, and well aligned and organized nanotube arrays were obtained [22]. Lei et al. reported that the photovoltaic performance of DSSCs based on TNT arrays on FTO glass reached 8.07%, which is higher than that of a TiO_2 nanoparticle electrode [23]. These reports all indicate that the fabrication of TNT arrays is a new potential approach for increasing the power conversion efficiency of DSSCs. In the study of TNT arrays, a variety of preparation methods

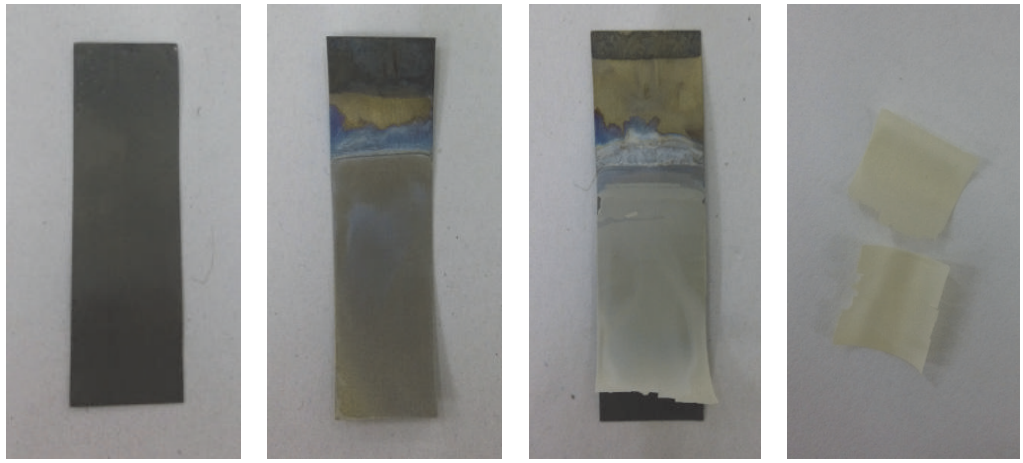

(a) (b) (c) (d)

Figure 1: The appearance of TiO_2 nanotube arrays in different stages of the preparation process: (a) Ti foil before treatment, (b) TNT arrays after the first anodization, (c) TNT arrays after second anodization, and (d) TNT arrays film eventually obtained.

are developed, such as hydrothermal method [24, 25], sol-gel method [26, 27], and electrochemical anodization [28–30]. Among all the methods for preparation of TNT arrays, the electrochemical anodization has the advantages of low cost, simple equipment, and easy process [31, 32]. The preparation of TNT arrays by electrochemical anodization method is a typical two-electrode system; the length, diameter, and wall thickness of nanotubes are closely related to anodization voltage and time. In addition, reports have shown that DSSCs with composite photoanode showed the best conversion efficiency. Zheng et al. reported that a combined structure with a mixture of TiO_2 nanotubes and nanoparticles was fabricated, and a high efficiency of 5.75% was achieved [33]. Accordingly, the synthesis of the composite photoanodes which were composed of various TiO_2 structures is an effective way to enhance the efficiency of DSSCs.

In this work, we fabricated a TiO_2 double-layer photoanode consisting of TNT arrays and TiO_2 nanoparticle (P25) for application in dye-sensitized solar cells. The crystallized TNT arrays films were prepared by using a two-step anodization technique. And TNT arrays film as overlayer can promote the transmission of electrons and reduces the recombination of electrons and holes. P25 has excellent capacity of dye adsorption and offers good contact between TNT arrays and FTO glass. In order to study the impact of TNT arrays with different morphologies on the performance of DSSCs, the preparation conditions of electrochemical anodization method were optimized. As a result, the photoelectronic conversion efficiency (PCE) of 4.20% was achieved in double-layer photoanode at 18 h, with an open-circuit voltage (V_{oc}) of 0.65 V and short-circuit current density (J_{sc}) of 9.98 mA cm^{-2}.

2. Experiment

2.1. Preparation of the TiO_2 Nanotube Arrays. TiO_2 nanotube arrays (TNT arrays) films were prepared by anodization of Ti foils (0.25 mm thickness, 99.7% purity) in an NH_4F/ethylene glycol electrolyte solution by using a DC power source. There are a lot of impurities on the surface of titanium, so the Ti foils were first degreased by chemical polishing solution before anodization. The chemical polishing solution was composed of deionized water, hydrogen nitrate, and hydrofluoric acid in volume ratio of 5 : 4 : 1. Then, the first anodization was carried out in the ethylene glycol electrolyte solution containing 0.5 wt% NH_4F and 3 vol% deionized water, while voltage of 50 V was applied versus a Pt counter electrode for different time (5 h, 12 h, 18 h, and 22 h). The as-anodized TNT arrays/Ti substrate was rinsed with DI water and ethanol and then annealed in an air furnace at 450°C for 30 min to form a crystalline structure. And the microstructure parameters of TNT arrays are slightly different due to the change of anodization time. Then, the as-anodized Ti foil was re anodized under the same conditions as the first anodization, and whether the TNT arrays film was separated from the Ti substrate carefully observed. After about an hour or so, the free-standing TNT arrays could be easily removed from the Ti substrate. The appearance of TiO_2 nanotube arrays in different stages of the preparation process is shown in Figure 1.

2.2. Fabrication of DSSCs Substance. In order to prepare the P25/TNT arrays composite film of photoelectrode, firstly, the P25 nanoparticle paste was pasted onto the FTO glass by using doctor-blade technique. Then the TNT arrays films were divided into 4 mm × 4 mm thin films and transferred onto the P25 underlayer immediately. After being dried in air, the double-layer composite films (active area, 4 mm × 4 mm) were annealed at 450°C for 30 min in a furnace.

After that, the as-prepared photoelectrodes were immersed into a 0.5 mM ethanol solution of N719 at room temperature and avoided light for 24 h. After being dried naturally, the three sides of the sensitized photoanodes were pasted with scotch tape, and then the photoanode

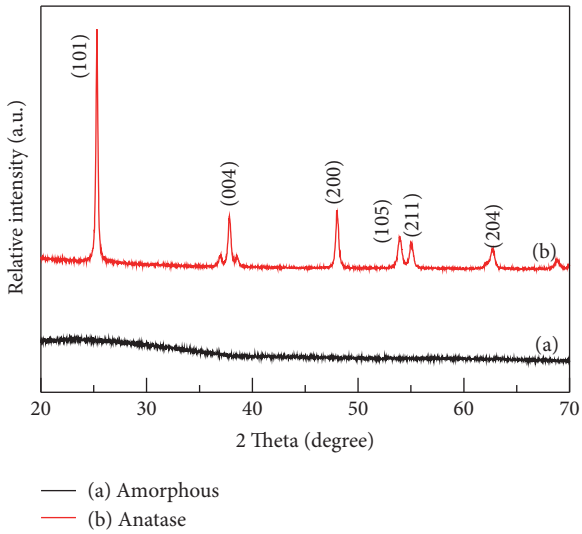

Figure 2: XRD patterns of TNT arrays before and after annealing.

and Pt counter electrode were clamped together by a clamp. The electrolyte (0.5 M LiI, 0.05 M I_2, 0.5 M 4-tert-butylpyridine, and 0.3 M 1,2-dimethyl-3-propylimidazolium iodide (DMPII) in dry acetonitrile) was injected into the edge without scotch tape of cell and absorbed into the inner space of cell, and the assembled cell was tested immediately.

2.3. Characterization and Measurements. X-ray powder diffraction (XRD) is one of the common test means in the analysis of material structure. The test instrument used in this paper is D/MAX-RB RU-200B target X-ray diffractometer produced by Rigaku. The morphology of the as-prepared samples was characterized by scanning electron microscopy (SEM, JSM-IT300, JEOL, Japan) and transmission electron microscopy (TEM, JEM-2100F, JEOL, Japan). The microscopic imaging of the material can be obtained by focusing the electron beam on the surface of the sample by point-by-point scanning in SEM. And the size and crystal state of the samples were observed by focusing the electron beam through the sample in TEM. The absorption spectra of the samples in a certain wavelength range can be tested by UV-vis spectrophotometer (UV-3600, Shimadzu, Japan). The photoelectric properties of the DSSCs are mainly analyzed by current-voltage (J-V) characteristics and electrochemical impedance spectra (EIS). The photocurrent-voltage (J-V) and EIS were studied by an electrochemical workstation (IM6, Germany) under AM 1.5 G solar simulator (100 mWcm^{-2}) provided by a solar light simulator (Oriel Sol3A, Newport Corporation, USA). The impedance parameters were obtained by fitting the equivalent circuit of Nyquist graph using Z-view software.

3. Results and Discussion

3.1. Phase Structures. Figure 2 shows XRD patterns of TNT arrays before and after annealing. As exhibited in Figure 2(a), the XRD pattern of as-anodized TNT arrays only shows the peak of Ti. It suggests that the TNT arrays have an amorphous structure before annealing. After calcinations at 450°C for 30 min, the strongest diffraction peak 2θ = 25.3° of TNT arrays is the characteristic diffraction peaks of anatase TiO_2, and other diffraction peaks were indexed to the standard anatase phase of TiO_2 (JCPDS card number: 21-1272). Through the XRD analyses, we can see that the phase structure of TNT arrays changes from amorphous structure to anatase structure by annealing at 450°C. Research shows that the anatase structure of TiO_2 has better photocatalytic activity than other crystal structures [34–36].

3.2. Microstructure and Morphology. Figures 3(a)–3(c) show typical SEM images of as-prepared TNT arrays film in a top view, bottom view, and cross-sectional view, respectively. It can be seen that the nanotubes opened on the top but closed on the bottom, and the distribution of nanotubes is highly ordered. The cross-sectional SEM image of double-layer film was shown in Figure 3(d), from which the double-layer structure of photoanode can be clearly seen. The fabrication procedure of the double-layer structure is shown in Figure 4. The bottom layer of the composite structure is P25 nanoparticles and the thickness is 9 μm. As a compact layer between the TNT arrays film and the FTO glass, P25 nanoparticle underlayer will enlarge contact area between them and reduce the occurrence of dark current. Studies have shown that TiO_2 composite films combined the characteristics of different TiO_2 nanostructures and achieved the higher conversion efficiency [37, 38]. As the overlayer of composite film, the TNT arrays film greatly improves the photoelectric properties of DSSCs. First of all, the unique structure of TiO_2 nanotube arrays provides a good channel for electron transfer and facilitates electron transport in the TiO_2 photoelectrode. Second, the presence of channel accelerates the penetration of the dye molecules into the deep film electrode, which increases the adsorption amount of dye. Finally, the electrolyte solution has a high rate of diffusion and metastases, which facilitate the process of electronic cycle.

In order to study the influence of anodization time on the micrographs of TNT arrays, anodization experiments at different anodization time (5 h, 12 h, 18 h, and 22 h) were performed under the same external experimental conditions. The cross-sectional SEM images of double-layer film with different anodization time were shown in Figure 5. As shown in Figure 5, the length of nanotubes increased from 7.13 um to 30 μm with increasing the anodization time from 5 h to 22 h. The influence of anodization time on TNT arrays is mainly reflected in the following two aspects. (1) When the anodization time is not enough, there is a part of the titanium substrate that has not yet formed a complete morphology of TiO_2 nanotubes. (2) The anodization time is the key factor to control the length of nanotubes. Therefore, it is very necessary to fabricate the high quality TNT arrays by controlling the anodization time reasonably.

3.3. UV-Visible Absorbed Spectra. The light-absorption capability of double-layer photoelectrode has great influence on

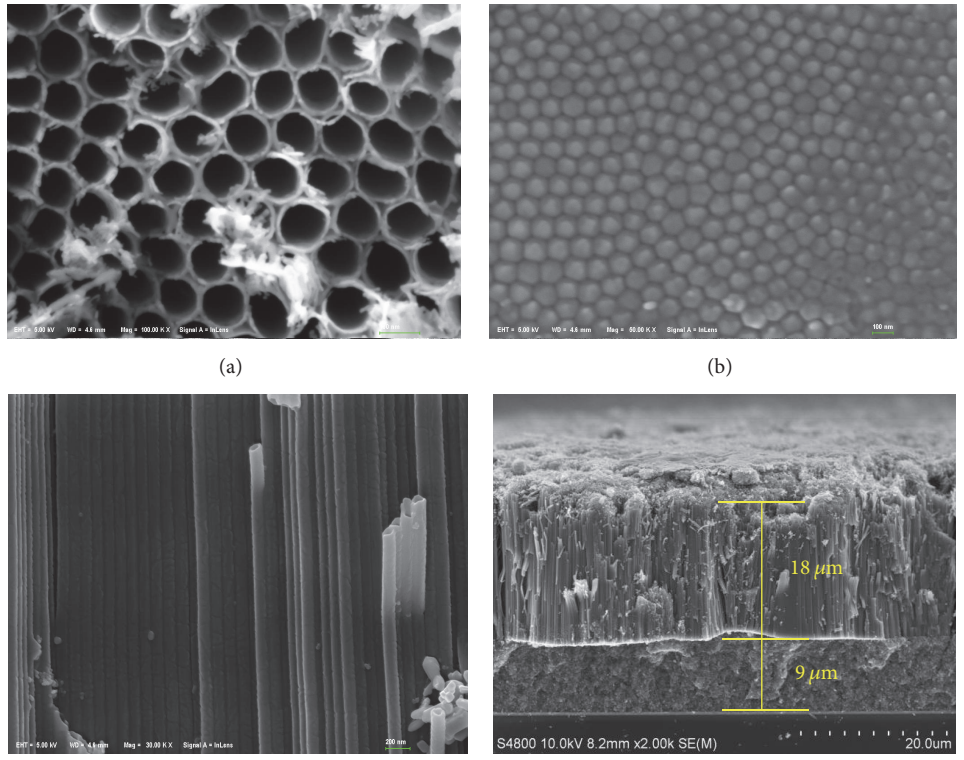

FIGURE 3: SEM images of TiO_2 nanotube arrays in (a) top view, (b) bottom view, and (c) cross-sectional view; (d) SEM image of double-layer composite film.

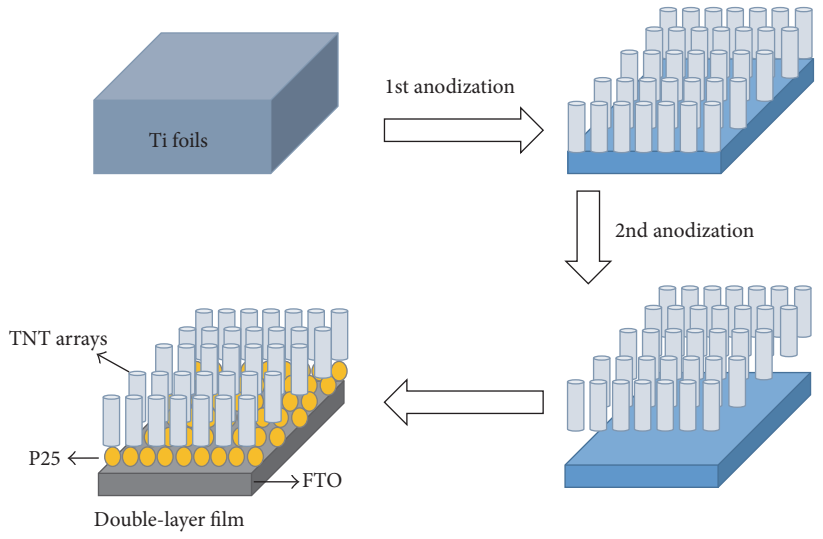

FIGURE 4: Schematic illustrating the fabrication process of P25/TNT arrays double-layer composite film.

the photoelectric performance of DSSCs [39, 40]. The absorption spectra of composite films at different anodization time were shown in Figure 6. It can be seen that the absorption peak of TiO_2 photoelectrode is located in 370 nm, and there is a light-absorption edge at the wavelength of 200 nm–300 nm. It is found that, with the increase of anodization time, the light-absorption edge of TiO_2 photoelectrode first increases and then decreases and reaches the peak at 18 h. The thickness of thin film increased with the increase of time, thereby promoting the adsorption of dye molecules. However, when the anodization time is too long, the covering on the surface of nanotubes will restrain the entry of sunlight. Therefore, the microstructure of TNT arrays with anodization time of 18 h is beneficial to the absorption of light.

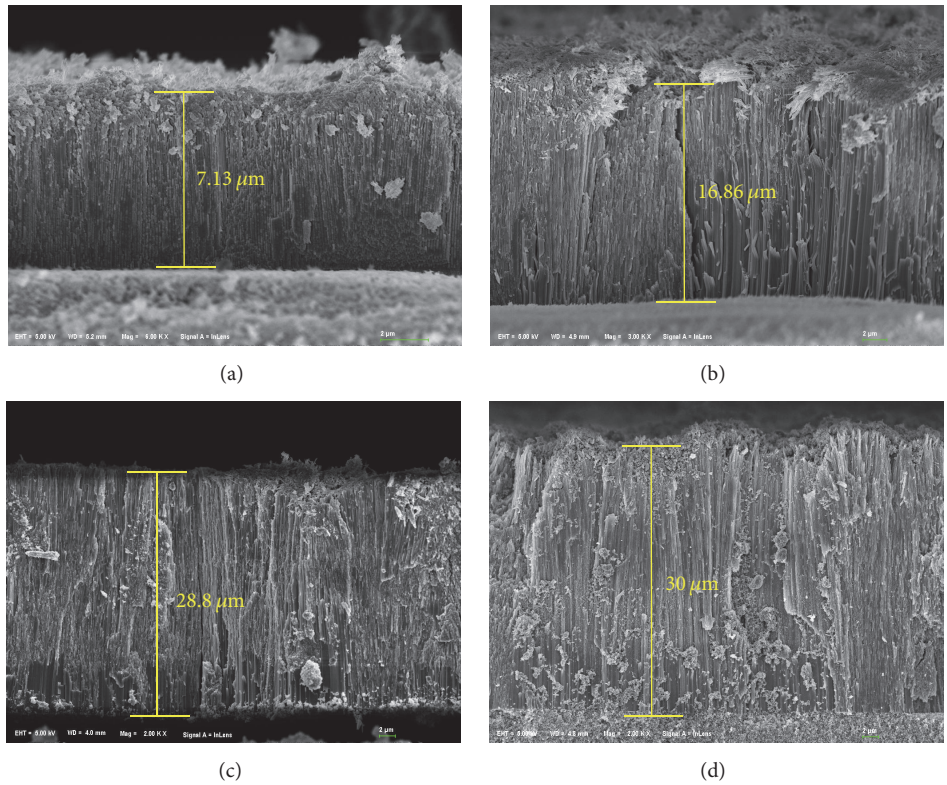

Figure 5: The cross-sectional SEM images of double-layer film with different anodization time: (a) 5 h, (b) 12 h, (c) 18 h, (d) and 22 h.

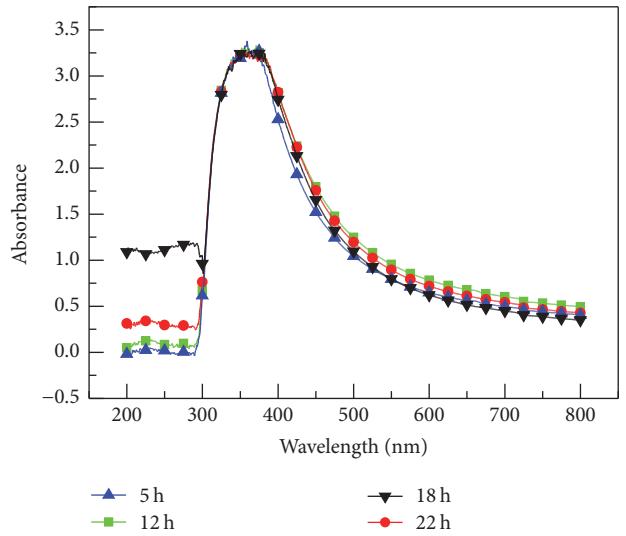

Figure 6: Absorption spectra of TiO_2 photoelectrodes based on P25/TNT arrays double-layer films at different anodization time.

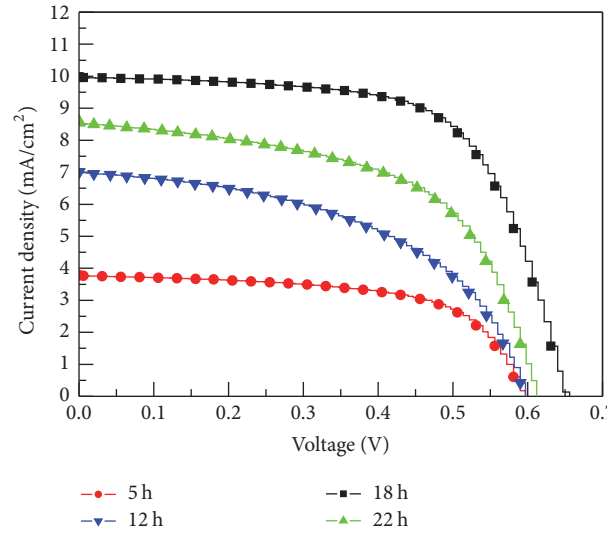

Figure 7: *I-V* performance of the DSSCs based on P25/TNT arrays double-layer films with different anodization time under AM 1.5 illuminations.

3.4. Photovoltaic Performances of DSSCs. Figure 7 shows the photocurrent density-photovoltage (*J-V*) of DSSCs based on TNT arrays film with different anodization time under AM 1.5 illuminations. The short-circuit current density (J_{sc}) and open-circuit voltage (V_{oc}) can be obtained directly from the *J-V* characteristic curve. And we can further calculate the fill factor (FF) and conversion efficiency (η) according to J_{sc} and V_{oc}, which were summarized in Table 1. According to the curve in Figure 7 and the data in Table 1, the conversion efficiency (η) of DSSCs can reach the maximum value of 4.20% in 18 hours of anodization and reach the minimum value of 1.39% in 5 hours of anodization. The increase of the thickness of the film ensures that the photoelectrode has a

Table 1: Comparisons of the photovoltaic performances of DSSCs based on P25/TNT arrays double-layer films with different anodization time.

Anodization time (h)	J_{sc} (mA/cm^2)	V_{oc} (V)	FF	η (%)
5 h	3.74	0.59	0.63	1.39
12 h	7.00	0.60	0.50	2.07
18 h	9.98	0.65	0.65	4.20
22 h	8.51	0.61	0.57	2.96

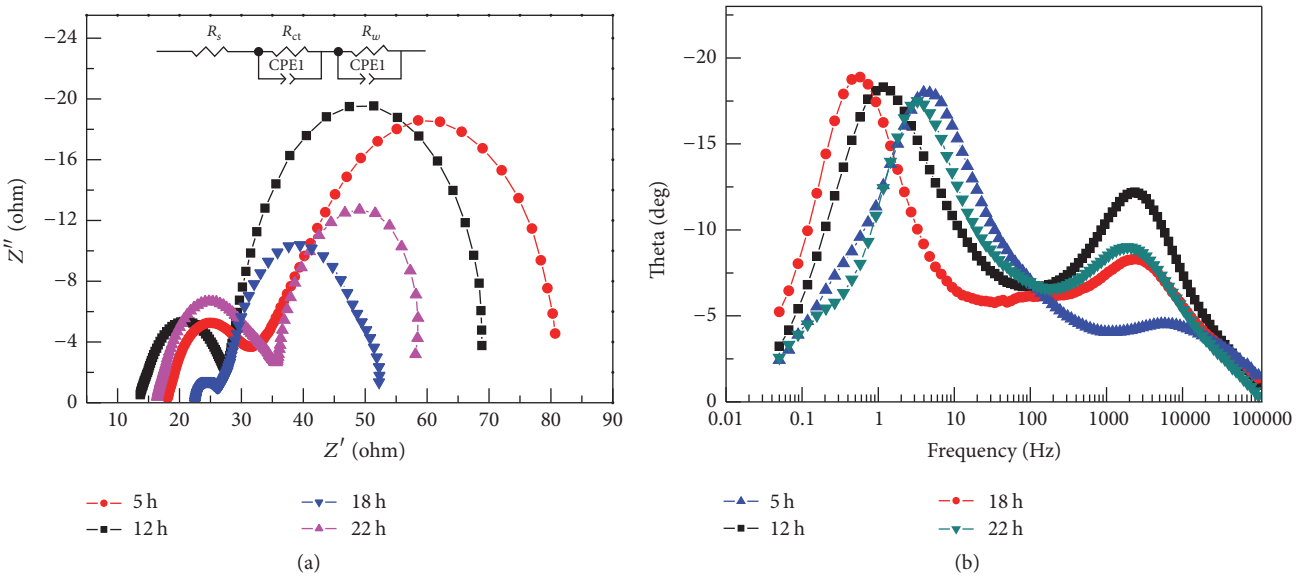

Figure 8: EIS spectra of the DSSCs based on P25/TNT arrays double-layer films with different anodization time. (a) Nyquist plots. (b) Bode phase plots.

large enough surface to adsorb the dye molecules, and the photoelectric conversion efficiency of DSSCs is improved [41]. However, when the thickness of the film is too thick, the transmission of electrons and the diffusion of electrolyte will slow down, which leads to the reduction of conversion efficiency. Therefore, there exists an anodization time to make the electrode in an optimum film thickness, and DSSCs have the best photoelectric performance. Hence, the photovoltaic performance of DSSCs firstly increases and then decreases with the increase of anodization time. Finally, a highest overall conversion efficiency of 4.20% is achieved for a TiO_2 composite film at 18 h, with short-circuit current density (J_{sc}) of 9.98 mA cm^{-2}, open-circuit voltage (V_{oc}) of 0.65 V, and fill factor (FF) of 0.65.

3.5. EIS Analysis. In order to further study the electron transport characteristics of DSSCs based on TNT arrays film with different anodization time, the electrochemical impedance spectroscopy (EIS) was performed under one-sun illumination and the resulting graphs were shown in Figure 8. As shown in Figure 8(a), two semicircles were shown in Nyquist plots at the frequency range of 10^{-2}–10^5 Hz, which represent two different charge transport processes [42, 43]. The equivalent circuit diagram is shown in the inset of Figure 8(a), from which we can obtain R_s, R_{ct}, and R_w by using Z-view software. R_s consisted of the contact resistance of TiO_2/FTO and the plane resistance of FTO. R_{ct} is the charge-transfer resistance of redox electrolyte/Pt electrode interface. R_w is associated with the electron transfer within TiO_2 film and the interfaces of TiO_2/redox electrolyte. R_s, R_{ct}, and R_w data with different anodization time are listed in Table 2. Obviously, from Table 2, we can see that TiO_2 composite film with anodization time of 18 h has the lowest values for R_{ct} and R_w resistance, which are 26.63 Ω and 26.45 Ω, respectively. These results indicate that the TiO_2/electrolyte interfaces and the electrolyte/Pt electrode interfaces of composite film with anodization time of 18 h have more efficient electron transport.

Table 2: Parameters obtained by fitting the impedance spectra of DSSCs using the equivalent circuit in Figure 8(a).

	5 h	12 h	18 h	22 h
R_s (Ω)	23.48	20.06	24.52	25.48
R_{ct} (Ω)	30.87	27.15	26.63	34.54
R_w (Ω)	59.41	45.42	26.45	28.21
τ_e (ms)	34.62	133.36	279.36	47.89

Figure 8(b) shows the Bode phase plots of EIS spectra, which display the frequency peaks of different charge-transfer process. The electron lifetime (τ_e) of DSSCs at different anodization time can be calculated by using the following equation: $\tau_e = 1/2\pi f_{\max}$ [44], where $f_{\max}$ is the maximum frequency of the low-frequency peak. As is shown in Table 2, the electron lifetime (τ_e) of DSSCs with anodization time of 18 h is longer than other films. Having a longer electron lifetime to ensure the occurrence of electronic cycle is another reason why TiO_2 composite film at 18 h has the highest conversion efficiency.

4. Conclusions

In conclusion, we have successfully fabricated TNT arrays films with different anodization time by two-step anodization process. And double-layer photoanodes with TiO_2 nanoparticles (P25) as the underlayer and TiO_2 nanotube arrays (TNT arrays) as overlayer film have been fabricated for application in DSSCs. The experiment results demonstrate that the length of TiO_2 nanotube arrays is closely related to anodization time and TiO_2 composite film DSSCs achieved the highest conversion efficiency of 4.20% when the anodization time is 18 h. Thus, higher-performance DSSCs were obtained by optimizing the preparation conditions.

Competing Interests

The authors declare that they have no competing interests.

Acknowledgments

This work was supported by the NSFC (51572072 and 11204070) and the Ph.D. Programs Foundation of Ministry of Educational of China (20114208110004). This work was also financially supported by Wuhan Science and Technology Bureau of Hubei Province of China (2013010602010209), Educational Commission of Hubei Province of China (D20141006), and Department of Science & Technology of Hubei Province of China (2015CFA118). This work was also financially supported by State Key Laboratory of Advanced Technology for Materials Synthesis and Processing (2016-KF-13).

References

[1] B. O'Regan and M. Grätzel, "A low-cost, high-efficiency solar cell based on dye-sensitized colloidal TiO_2 films," *Nature*, vol. 353, no. 6346, pp. 737–740, 1991.

[2] Y. Chiba, A. Islam, Y. Watanabe, R. Komiya, N. Koide, and L. Han, "Dye-sensitized solar cells with conversion efficiency of 11.1%," *Japanese Journal of Applied Physics*, vol. 45, no. 24–28, pp. L638–L640, 2006.

[3] R. Jose, V. Thavasi, and S. Ramakrishna, "Metal oxides for dye-sensitized solar cells," *Journal of the American Ceramic Society*, vol. 92, no. 2, pp. 289–301, 2009.

[4] A. Mathew, G. M. Rao, and N. Munichandraiah, "Dye sensitized solar cell based on platinum decorated multiwall carbon nanotubes as catalytic layer on the counter electrode," *Materials Research Bulletin*, vol. 46, no. 11, pp. 2045–2049, 2011.

[5] Y. Kondo, H. Yoshikawa, K. Awaga et al., "Preparation, photocatalytic activities, and dye-sensitized solar-cell performance of submicron-scale TiO_2 hollow spheres," *Langmuir*, vol. 24, no. 2, pp. 547–550, 2008.

[6] H. Sun, D. Qin, S. Huang et al., "Dye-sensitized solar cells with NiS counter electrodes electrodeposited by a potential reversal technique," *Energy and Environmental Science*, vol. 4, no. 8, pp. 2630–2637, 2011.

[7] G. Yue, J. Wu, J.-Y. Lin et al., "A counter electrode of multi-wall carbon nanotubes decorated with tungsten sulfide used in dye-sensitized solar cells," *Carbon*, vol. 55, pp. 1–9, 2013.

[8] J. Van De Lagemaat, N.-G. Park, and A. J. Frank, "Influence of electrical potential distribution, charge transport, and recombination on the photopotential and photocurrent conversion efficiency of dye-sensitized nanocrystalline TiO_2 Solar Cells: A Study by Electrical Impedance and Optical Modulation Techniques," *Journal of Physical Chemistry B*, vol. 104, no. 9, pp. 2044–2052, 2000.

[9] M. Hocevar, M. Berginc, M. Topič, and U. O. Krašovec, "Sponge-like TiO_2 layers for dye-sensitized solar cells," *Journal of Sol-Gel Science and Technology*, vol. 53, no. 3, pp. 647–654, 2010.

[10] K.-M. Lee, V. Suryanarayanan, and K.-C. Ho, "A study on the electron transport properties of TiO_2 electrodes in dye-sensitized solar cells," *Solar Energy Materials and Solar Cells*, vol. 91, no. 15-16, pp. 1416–1420, 2007.

[11] S. J. Li, Y. Lin, Z. Chen, J. B. Zhang, and X. W. Zhou, "Electrochemical impedance analysis of nanoporous TiO_2 electrode at low bias potential," *Chinese Chemical Letters*, vol. 21, no. 8, pp. 959–962, 2010.

[12] Z. Li, K. Shankar, G. K. Mor et al., "Functionalized pentacenes for dye-sensitized solar cells," *Journal of Photonics for Energy*, vol. 1, no. 1, Article ID 11106, 2011.

[13] A. Kay and M. Grätzel, "Dye-sensitized core-shell nanocrystals: improved efficiency of mesoporous tin oxide electrodes coated with a thin layer of an insulating oxide," *Chemistry of Materials*, vol. 14, no. 7, pp. 2930–2935, 2002.

[14] H. Xu, X. Tao, D.-T. Wang, Y.-Z. Zheng, and J.-F. Chen, "Enhanced efficiency in dye-sensitized solar cells based on TiO2 nanocrystal/nanotube double-layered films," *Electrochimica Acta*, vol. 55, no. 7, pp. 2280–2285, 2010.

[15] Y. Shi, L. Zhao, S. Wang et al., "Double-layer composite film based on hollow TiO_2 boxes and P25 as photoanode for enhanced efficiency in dye-sensitized solar cells," *Materials Research Bulletin*, vol. 59, pp. 370–376, 2014.

[16] G. Dai, L. Zhao, S. Wang et al., "Double-layer composite film based on sponge-like TiO_2 and P25 as photoelectrode for enhanced efficiency in dye-sensitized solar cells," *Journal of Alloys and Compounds*, vol. 539, pp. 264–270, 2012.

[17] B. Liu and E. S. Aydil, "Growth of oriented single-crystalline rutile TiO_2 nanorods on transparent conducting substrates for dye-sensitized solar cells," *Journal of the American Chemical Society*, vol. 131, no. 11, pp. 3985–3990, 2009.

[18] X. Feng, K. Shankar, O. K. Varghese, M. Paulose, T. J. Latempa, and C. A. Grimes, "Vertically aligned single crystal TiO_2 nanowire arrays grown directly on transparent conducting oxide coated glass: synthesis details and applications," *Nano Letters*, vol. 8, no. 11, pp. 3781–3786, 2008.

[19] L. Zhao, J. Yu, J. Fan, P. Zhai, and S. Wang, "Dye-sensitized solar cells based on ordered titanate nanotube films fabricated

by electrophoretic deposition method," *Electrochemistry Communications*, vol. 11, no. 10, pp. 2052–2055, 2009.

[20] K. Zhu, N. R. Neale, A. Miedaner, and A. J. Frank, "Enhanced charge-collection efficiencies and light scattering in dye-sensitized solar cells using oriented TiO_2 nanotubes arrays," *Nano Letters*, vol. 7, no. 1, pp. 69–74, 2007.

[21] J. Lee, K. S. Hong, K. Shin, and J. Y. Jho, "Fabrication of dye-sensitized solar cells using ordered and vertically oriented TiO_2 nanotube arrays with open and closed ends," *Journal of Industrial and Engineering Chemistry*, vol. 18, no. 1, pp. 19–23, 2012.

[22] D. Gong, C. A. Grimes, O. K. Varghese et al., "Titanium oxide nanotube arrays prepared by anodic oxidation," *Journal of Materials Research*, vol. 16, no. 12, pp. 3331–3334, 2001.

[23] B.-X. Lei, J.-Y. Liao, R. Zhang, J. Wang, C.-Y. Su, and D.-B. Kuang, "Ordered crystalline TiO_2 nanotube arrays on transparent FTO glass for efficient dye-sensitized solar cells," *The Journal of Physical Chemistry C*, vol. 114, no. 35, pp. 15228–15233, 2010.

[24] S. Sreekantan and L. C. Wei, "Study on the formation and photocatalytic activity of titanate nanotubes synthesized via hydrothermal method," *Journal of Alloys and Compounds*, vol. 490, no. 1-2, pp. 436–442, 2010.

[25] K.-P. Yu, W.-Y. Yu, M.-C. Kuo, Y.-C. Liou, and S.-H. Chien, "Pt/titania-nanotube: a potential catalyst for CO_2 adsorption and hydrogenation," *Applied Catalysis B: Environmental*, vol. 84, no. 1-2, pp. 112–118, 2008.

[26] T. Maiyalagan, B. Viswanathan, and U. V. Varadaraju, "Fabrication and characterization of uniform TiO_2 nanotube arrays by sol-gel template method," *Bulletin of Materials Science*, vol. 29, no. 7, pp. 705–708, 2006.

[27] T.-S. Kang, A. P. Smith, B. E. Taylor, and M. F. Durstock, "Fabrication of highly-ordered TiO_2 nanotube arrays and their use in dye-sensitized solar cells," *Nano Letters*, vol. 9, no. 2, pp. 601–606, 2009.

[28] J. M. Macak and P. Schmuki, "Anodic growth of self-organized anodic TiO_2 nanotubes in viscous electrolytes," *Electrochimica Acta*, vol. 52, no. 3, pp. 1258–1264, 2006.

[29] A. E. R. Mohamed and S. Rohani, "Modified TiO_2 nanotube arrays (TNTAs): progressive strategies towards visible light responsive photoanode, a review," *Energy and Environmental Science*, vol. 4, no. 4, pp. 1065–1086, 2011.

[30] R. V. Chernozem, M. A. Surmeneva, and R. A. Surmenev, "Influence of anodization time and voltage on the parameters of TiO_2 nanotubes," *IOP Conference Series: Materials Science and Engineering*, vol. 116, Article ID 012025, 2016.

[31] J. Hu, L. Zhao, Y. Yang et al., "TiO_2 nanotube arrays composite film as photoanode for high-efficiency dye-sensitized solar cell," *International Journal of Photoenergy*, vol. 2014, Article ID 602692, 8 pages, 2014.

[32] P.-T. Hsiao, Y.-J. Liou, and H. Teng, "Electron transport patterns in TiO_2 nanotube arrays based dye-sensitized solar cells under frontside and backside illuminations," *The Journal of Physical Chemistry C*, vol. 115, no. 30, pp. 15018–15024, 2011.

[33] D. Zheng, M. Lv, S. Wang, W. Guo, L. Sun, and C. Lin, "A combined TiO_2 structure with nanotubes and nanoparticles for improving photoconversion efficiency in dye-sensitized solar cells," *Electrochimica Acta*, vol. 83, no. 12, pp. 155–159, 2012.

[34] Y. Lai, L. Sun, Y. Chen, H. Zhuang, C. Lin, and J. W. Chin, "Effects of the structure of TiO_2 nanotube array on Ti substrate on its photocatalytic activity," *Journal of the Electrochemical Society*, vol. 153, no. 7, pp. D123–D127, 2006.

[35] A. M. Bakhshayesh, M. R. Mohammadi, and D. J. Fray, "Controlling electron transport rate and recombination process of TiO_2 dye-sensitized solar cells by design of double-layer films with different arrangement modes," *Electrochimica Acta*, vol. 78, pp. 384–391, 2012.

[36] H.-G. Jung, Y. S. Kang, and Y.-K. Sun, "Anatase TiO_2 spheres with high surface area and mesoporous structure via a hydrothermal process for dye-sensitized solar cells," *Electrochimica Acta*, vol. 55, no. 15, pp. 4637–4641, 2010.

[37] J. Yao, C.-M. Lin, S. Yin, P. Ruffin, C. Brantley, and E. Edwards, "High open-circuit voltage dye-sensitized solar cells based on a nanocomposite photoelectrode," *Journal of Photonics for Energy*, vol. 5, no. 1, Article ID 053088, 2015.

[38] J. Hu, J. Cheng, S. Tong, L. Zhao, J. Duan, and Y. Yang, "Dye-sensitized solar cells based on P25 nanoparticles/TiO_2, nanotube arrays/hollow TiO_2 boxes three-layer composite film," *Journal of Materials Science: Materials in Electronics*, vol. 27, no. 5, pp. 5362–5370, 2016.

[39] J. Yu, Q. Li, and Z. Shu, "Dye-sensitized solar cells based on double-layered TiO_2 composite films and enhanced photovoltaic performance," *Electrochimica Acta*, vol. 56, no. 18, pp. 6293–6298, 2011.

[40] Y. Lee, J. Chae, and M. Kang, "Comparison of the photovoltaic efficiency on DSSC for nanometer sized TiO_2 using a conventional sol-gel and solvothermal methods," *Journal of Industrial and Engineering Chemistry*, vol. 16, no. 4, pp. 609–614, 2010.

[41] R. Kern, R. Sastrawan, J. Ferber, R. Stangl, and J. Luther, "Modeling and interpretation of electrical impedance spectra of dye solar cells operated under open-circuit conditions," *Electrochimica Acta*, vol. 47, no. 26, pp. 4213–4225, 2002.

[42] D. Kuang, C. Klein, Z. Zhang et al., "Stable, high-efficiency ionic-liquid-based mesoscopic dye-sensitized solar cells," *Small*, vol. 3, no. 12, pp. 2094–2102, 2007.

[43] F. Fabregat-Santiago, J. Bisquert, E. Palomares et al., "Correlation between photovoltaic performance and impedance spectroscopy of dye-sensitized solar cells based on ionic liquids," *The Journal of Physical Chemistry C*, vol. 111, no. 17, pp. 6550–6560, 2007.

[44] S. M. Park and J. S. Yoo, "Electrochemical impedance spectroscopy for better electrochemical measurements," *Analytical Chemistry*, vol. 75, no. 21, pp. 455–461, 2003.